Dynamic Modelling, Simulation, and Model Predictive Control of a Tailings Treatment Surge Tank

J. J. Burchell[a,b], D. le Roux[b], I. K. Craig[b]

[a]*Sibanye-Stillwater, Johannesburg, South Africa*
[b]*Department of Electrical, Electronic and Computer Engineering, University of Pretoria, Pretoria, South Africa.*

Abstract

A dynamic model is derived to describe the rate of change of both volume and density for a tailings treatment surge tank. This model is validated using data from one of Sibanye-Stillwater's plants that stabilises tailings fed to a chrome recovery plant. Using the model simulations are was used to develop a non-linear model predictive controller for the plantsimulate the surge tank's response to multiple input density disturbances while under linear model predictive control. Compared to a simple control philosophy that relies only on a sizeable surge tank inventory to dampen input density disturbances, the model predictive controller was able to reduce output density fluctuations by a further 17 %.

Keywords: dynamic modelling, simulation, model predictive control

1. Introduction

Waste material from the primary processing of a metal ore is called tailings, and are typically stored in a dam formed by constructing a barrage from the tailings itself. The barrage is constructed at an angle for structural support, resulting in the dam taking on a trapezoidal shape.

In hard rock mining tailings consists of a fine particle slurry. When deposited in the dam the solids from the slurry settles to the bottom, and the water is recycled back to the process. To accomodate more waste the height of the dam is increased by extending the crest of the barrage.

In general, tailings are retreated to recover metals or minerals with sufficient economic value, to reclaim valuable land, or to mitigate safety and

environmental risks. This paper discusses the implementation of a non-linear model predictive controller (NMPC) to increase the recovery of chrome from a platinum group metals (PGM) tailings. This PGM tailings is owned and retreated by Sibanye-Stillwater in the Marikana area in the North West province of South Africa.

The development of the NMPC followed the general control problem (GCP) framework for developing advanced controllers (Craig, 1997; Craig and Henning, 2000), outlined in Fig. 1. The layout of this paper also follows the GCP framework. In section 2 the tailings retreatment circuit is studied for control purposes. A mathematical model is developed and validated in section 3. Using this model, a control design and analysis is performed in section 4, motivating for a NMPC control solution. An NMPC was implemented, and its performance is evaluated in section 5.

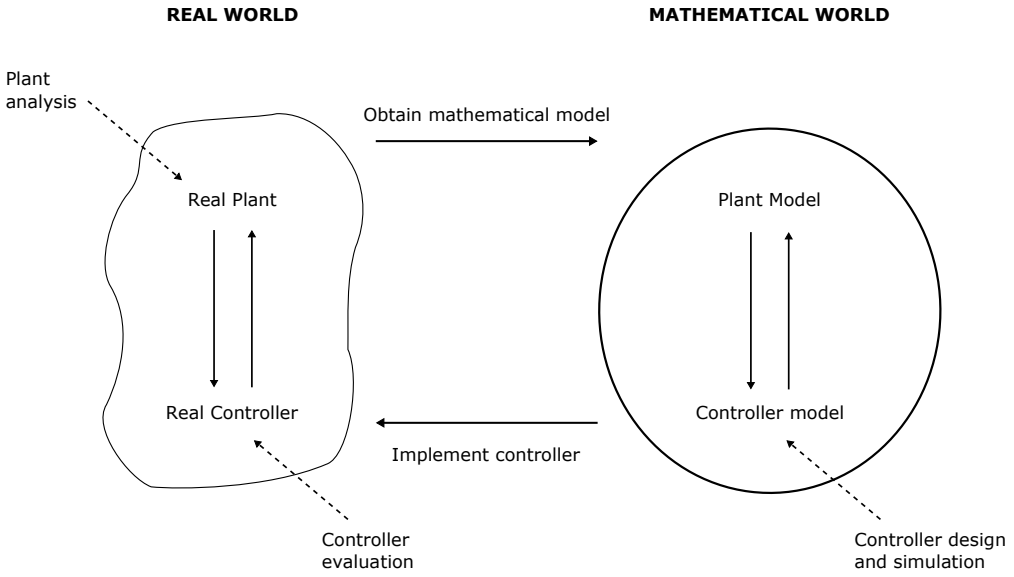

Figure 1: The general control framework for developing advanced control systems.

2. Circuit Analysis

Fig. 2 presents an overview of the circuit used to recover chrome from the tailings dam. A bulk tailings treatment (BTT) plant dewaters and stabilises the tailings before it is fed to a chrome concentrator plant. This concentrator

plant produces chrome using spiral separators, which sort the tailings into different chrome grades and a gangue waste product using gravity separation.

To assess the feasibility of this tailings retreatment project, and to motivate for its funding, the following factors were likely considered:

- The total amount of chrome in the dam, estimated from a geolocial survey.
- Characteristics of the tailings, such as its particle size distribution (PSD), also estimated by a geolocical survey.
- What recovery[1] would be achieved by the project. The recovery of the project would be influenced by tailings characteristics, such as the PSD, which would affect the efficiency of cyclones and spirals.
- What would be the operating throughput[2], which would largely be influenced by design considerations such as the sizing of pumps, spirals, thickeners, etc.
- The expected chrome price over the life of the project.
- The operating costs over the life of the project.

Using these factors an internal rate of return (IRR), an estimate of the profitability of the project, can be estimated. If the internal rate of return (IRR) for the project exceeds some minimum acceptable rate of return the project is deemed feasible.

Of the listed factors influencing the IRR for the project, recovery is by far the most affected by improving the control and operation of the circuit post its commissioning. The total amount of chrome in the dam, the tailings characteristics, and chrome price can not be influenced at all, while operating cost and throughput is largely influenced by circuit design. The key performance indicator for the chrome retreatment circuit is therefore its recovery. During the lifetime of the project, operations are continuously under

[1]Here *recovery* refers to the percentage of chrome in the tailings that would be recovered as product, with all unrecovered chrome lost to the gangue waste.

[2]Here *throughput* refers to the rate, in tons per hour, at which tailings would be processed by the circuit.

pressure to achieve a target recovery, and any improvements on this recovery is celebrated as a realisation of the upside potential for the project.

Ultimately, the recovery of the circuit depends on the efficiencies of the spiral separators, since they are the classifiers, sorting tailings into chrome product and gangue waste. Since the spiral separators' efficiencies are most sensitive to disturbances in density (Holland-Batt et al., 1982), the key control objective for the circuit must be to supply the chrome concentrator with a stable feed density.

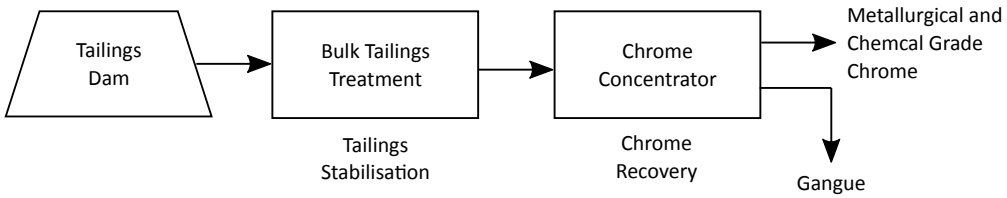

Figure 2: Chrome recovery circuit.

Fig. 3 presents an overview of the tailings dam operations. High pressure water is pumped from the BTT plant, and used to erode the dam into a tailings slurry. The tailings runs through naturally formed channels into a sump. This sump contains a floating barge and a vertical pump.

Two operators oversee re-mining operations at the tailings dam. The first manages the positioning of a high pressure hose that targets the tailings dam face, to adjust the density of the tailings supplied to the BTT plant. The second manages sump operations, and agitates the sump with high pressure water to avoid excessive settling of solids in the sump, which also affects the density of tailings to the BTT plant. The density of the tailings to the BTT plant is monitored by the BTT control room. Requests for density adjustment are communicated via hand radio to the tailings dam operators.

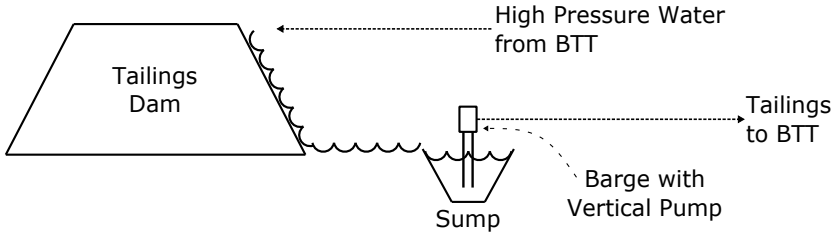

Figure 3: Flowsheet of the Tailings Dam operations.

An overview of the BTT plant's flowsheet is presented in Fig. 4. It uses a large vibrating screen to remove plant debris that unavoidably make its way into the tailings feed. A surge tank is then used to stabilise the tailings density, followed by a hydrocyclone and thickener for dewatering.

The overall performance of the plant is measured on the stability of the tailings from the holding tank. Since the feed density to a hydrocyclone has by far the largest impact on the hydrocyclone efficiency (Ntengwe and Witika, 2011), compounding improvements in both hydrocyclone and thickener efficiencies can be expected from stabilising the surge tank density. Hence, the work presented here focuses on improving the stability of the surge tank density.

3. Dynamic Modelling

3.1. Non-Linear state space model

A non-linear model of the surge tanks was developed to assess how effective different control strategies are at rejecting the typical input density disturbances from the tailing dam. Fig. 5 presents a simplified schematic diagram of the surge tank, with all relevant process variables labelled. The input flow rate, water flow rate, and output flow rate are respectively q_i, q_w,

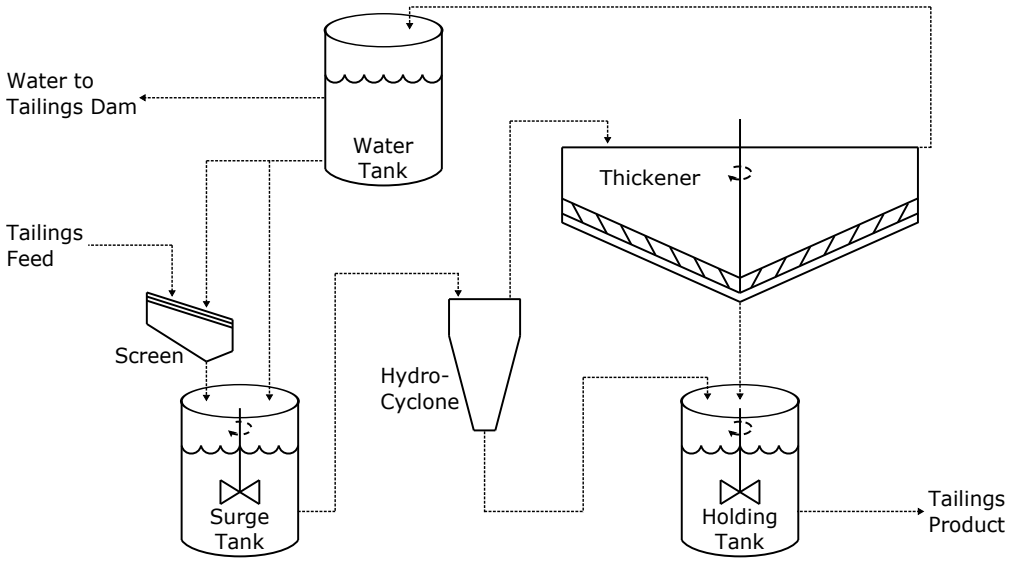

Figure 4: Flowsheet of the BTT plant.

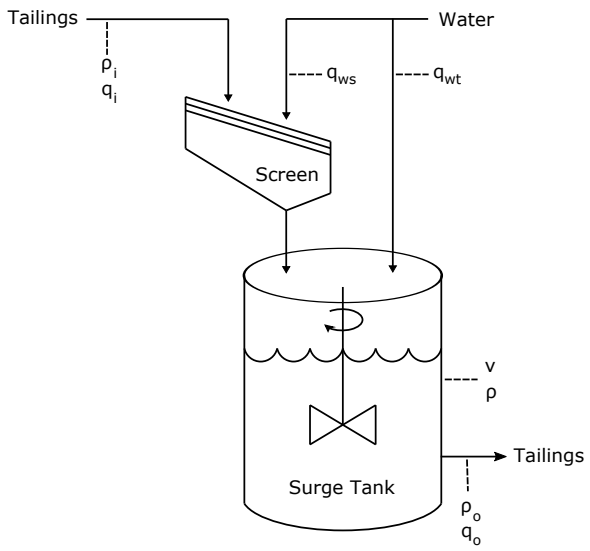

Figure 5: BTT surge tank.

and q_o.The tank volume, derived from a tank level measurement, is v, and the input density, the density in the tank, and the output density are ρ_i, ρ, and ρ_o.

Assuming perfect mixing, i.e. $\rho = \rho_o$, and conservation of mass the rate of accumulation of mass in the surge tank is

$$\frac{d\rho v}{dt} = \rho_i q_i + q_w - \rho q_o. \tag{1}$$

Table 1: A description of the surge tank process variables.

Parameter	Units	Description
q_i	m^3/h	Feed from tailings dam.
q_w	m^3/h	Total water to surge tank.
q_o	m^3/h	Tailings feed from surge tank.
ρ_i	$tons/m^3$	Input density from tailings dam.
ρ	$tons/m^3$	Density in surge tank.
ρ_o	$tons/m^3$	Output density from surge tank.
v	m^3	Volume in surge tank.

The differential term on the left is expanded using the chain rule

$$v\frac{d\rho}{dt} + \rho\frac{dv}{dt} = \rho_i q_i + q_w - \rho q_o. \tag{2}$$

Assuming no volume change during mixing, which is a reasonable assumption when modelling slurry dynamics (Dontsov and Perice, 2014), the volume in the surge tank will be conserved, and the rate of change of volume in the surge tank can be expressed as

$$\frac{dv}{dt} = q_i + q_w - q_o. \tag{3}$$

Substituting (3) into (2) gives the rate of accumulation of density independent of the rate of change in volume

$$\frac{d\rho}{dt} = \frac{q_i\rho_i - \rho(q_i + q_w) + q_w}{v}. \tag{4}$$

The non-linear model of the surge tank follows from (3) and (4)

$$\begin{bmatrix}\dot{v}\\ \dot{\rho}\end{bmatrix} = \begin{bmatrix} q_i + q_w - q_o \\ \frac{1}{v}(q_i\rho_i - \rho(q_i + q_w) + q_w)\end{bmatrix}, \tag{5}$$

which is of the form:

$$\dot{\boldsymbol{x}} = \boldsymbol{f}(\boldsymbol{x}, \boldsymbol{u}, \boldsymbol{d}). \tag{6}$$

For this problem, the elements of the state vector $\boldsymbol{x}$ is v and ρ, the elements of the input vector $\boldsymbol{u}$ are q_i and q_w, and the elements of the disturbance vector $\boldsymbol{d}$ are ρ_i and q_o.

3.2. Model Validation

The model in (5) is validated using a 10 hour long dataset collected from the plant while it was under normal operation, i.e. while the plant was not under start-up or shut-down. Fig. 6 provides an overview of this validation dataset.

Some interesting observations about plant dynamics and the baseline control strategy can be made from the dataset. Firstly, the input density varies at times rapidly, and generally over a large range, as expected due to the highly manual operation of the process at the tailing dam, as described in Section 2. Secondly, the input flow is inversely proportional to the input

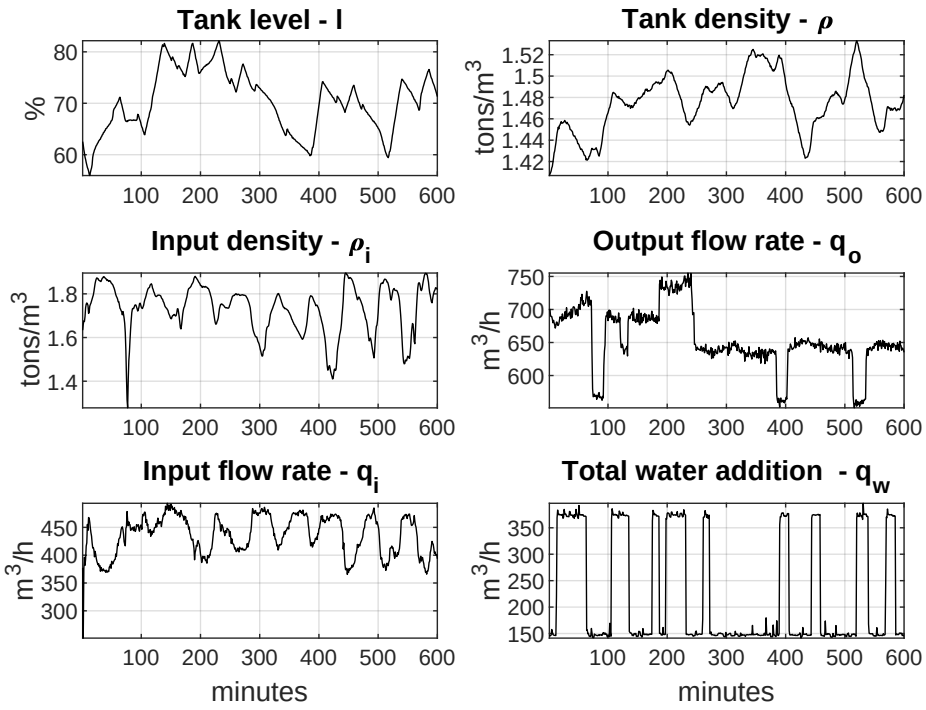

Figure 6: Data from time period when plant during normal operation.

density, which is as expected since there was no control element on the input line to surge tank at this time. Therefore, the flow dynamics would be dominated by density deviation, since the supply head would be inversely proportional to the input density.

As for insights into the baseline control strategy, clearly it implements steps in water addition and output flow rate to maintain tank level and tank density within unspecified ranges. On further investigation, the output flow rate is not directly adjusted to maintain tank level, there is actually a pressure controller on the output line, to keep the pressure across the hydrocyclone constant. The set-point to this pressure controller is stepped to affect a change in output flow, to maintain the tank level.

For model validation, the tank level and tank density was simulated over the complete dataset using the non-linear model, presented in (5). The simulated tank density and level is shown in Fig. 7, together with the measured signals from the dataset.

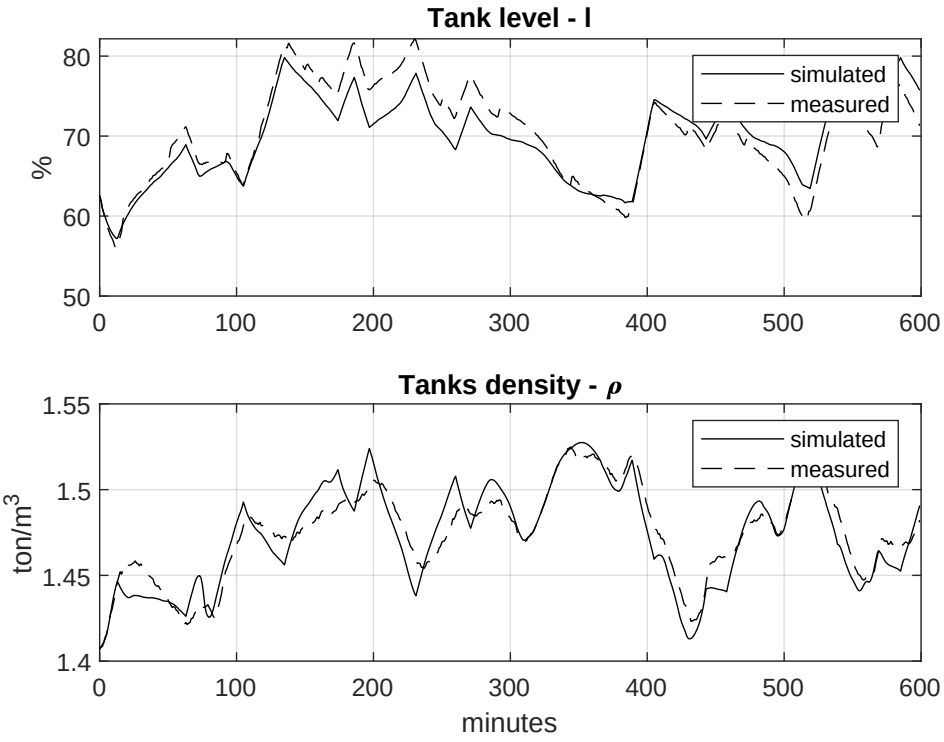

Figure 7: Validation of the non-linear model.

Clearly there is good correspondence. Small deviations between the measured and simulated tank levels can possibly be due to inaccurate instrument calibration, while deviation between simulated and measured tank density could also include inaccuracies due to the perfect mixing assumption.

3.3. Linear approximation

A linear approximation of a system is generally useful in that it allows for applying the well developed theory on linear systems (Skogestad and Postlethwaite, 2005) to gain insights into the system's dynamic behaviour. An in-depth exploration of the surge tank's dynamics is not presented here, however, the interested reader is referred to (XXXLuke's PaperXXX) wherein is included an input/output controllability analysis for this system. The linear approximation for the surge tank's dynamics is described here and used in the section that follows to motivate for the use of a non-linear model predictive control solution.

In general, a linear approximation for a non-linear system can be obtained by a Taylor series expansion of functions (Seborg et al., 2011). Consider the function $f(x)$ of a single variable x. The Taylor series expansion of $f(x)$ about the point $x = \bar{x}$ is

$$\begin{aligned} f(x) &= f(\bar{x}) + \left.\frac{\partial f}{\partial x}\right|_{\bar{x}} \delta x + \frac{1}{2} \left.\frac{\partial^2 f}{\partial x^2}\right|_{\bar{x}} \delta x^2 + \frac{1}{6} \left.\frac{\partial^3 f}{\partial x^3}\right|_{\bar{x}} \delta x^3 + ... \\ &= \sum_{n=0}^{\infty} \frac{1}{n!} \left.\frac{\partial^n f}{\partial x^n}\right|_{\bar{x}} \delta x^n, \end{aligned} \tag{7}$$

with $\delta x = x - \bar{x}$. For x close to $\bar{x}$ the higher order terms in (7) will be approximately zero. Hence, a linear approximation of $f(x)$ is obtained by discarding the higher order terms

$$f(x) \cong f(\bar{x}) + \left.\frac{\partial f}{\partial x}\right|_{\bar{x}} \delta x. \tag{8}$$

The expression for the accumulation of volume in (3) is already linear, therefore, a linear approximation of the surge tank requires only a Taylor series expansion of (4). Taking the functional form

$$\frac{d\rho}{dt} = f_\rho(q_i, q_w, q_o, \rho_i, \rho, v), \tag{9}$$

and applying a multivariate extension of (8) about the nominal steady-state operating point $\bar{x} = (\bar{q}_i, \bar{q}_w, \bar{\rho}_i, \bar{\rho}, \bar{v})$ gives:

$$\begin{aligned} f_\rho(q_i, q_w, q_o, \rho_i, \rho, v) \cong\ & f_\rho(\bar{x}) + \left.\frac{\partial f_\rho}{\partial q_i}\right|_{\bar{x}} \delta q_i + \left.\frac{\partial f_\rho}{\partial q_w}\right|_{\bar{x}} \delta q_w + \left.\frac{\partial f_\rho}{\partial q_o}\right|_{\bar{x}} \delta q_o + \\ & \left.\frac{\partial f_\rho}{\partial \rho_i}\right|_{\bar{x}} \delta \rho_i + \left.\frac{\partial f_\rho}{\partial \rho}\right|_{\bar{x}} \delta \rho + \left.\frac{\partial f_\rho}{\partial v}\right|_{\bar{x}} \delta v \end{aligned} \tag{10}$$

$$\begin{aligned} &\cong f_\rho(\bar{x}) + \frac{\bar{\rho}_i - \bar{\rho}}{\bar{v}} \delta q_i + \frac{1 - \bar{\rho}}{\bar{v}} \delta q_w + \frac{\bar{q}_i}{\bar{v}} \delta \rho_i \\ &\quad - \frac{\bar{q}_i + \bar{q}_w}{\bar{v}} \delta \rho - \frac{\bar{q}_i \bar{\rho}_i + \bar{q}_w - (\bar{q}_i + \bar{q}_w)\bar{\rho}}{\bar{v}^2} \delta v. \end{aligned}$$

By definition, at steady state

$$\begin{aligned} \bar{q}_i + \bar{q}_w - \bar{q}_o &= 0 \\ \text{and} & \\ \bar{q}_i \bar{\rho}_i + \bar{q}_w - \bar{q}_o \bar{\rho} &= 0, \end{aligned} \tag{11}$$

and (10) reduces to:

$$f_\rho(q_i, q_w, q_o, \rho_i, \rho, v) \cong f_\rho(\bar{x}) + \frac{\bar{\rho}_i - \bar{\rho}}{\bar{v}}\delta q_i + \frac{1-\bar{\rho}}{\bar{v}}\delta q_w + \frac{\bar{q}_i}{\bar{v}}\delta\rho_i - \frac{\bar{q}_o}{\bar{v}}\delta\rho. \quad (12)$$

A linear approximation of the surge tank model follows from (3) and (12), presented here in state space form:

$$\begin{aligned} \dot{\boldsymbol{x}} &= \boldsymbol{A}\boldsymbol{x} + \boldsymbol{B}\boldsymbol{u} \\ \boldsymbol{y} &= \boldsymbol{C}\boldsymbol{x} \\ &\text{with} \\ \dot{\boldsymbol{x}} = \begin{bmatrix} \frac{dv}{dt} \\ \frac{d\rho}{dt} \end{bmatrix}, \boldsymbol{x} &= \begin{bmatrix} v \\ \rho \end{bmatrix}, \boldsymbol{u} = \begin{bmatrix} q_i \\ q_w \\ q_o \\ \rho_i \end{bmatrix}, \end{aligned} \quad (13)$$

$$\boldsymbol{A} = \begin{bmatrix} 0 & 0 \\ 0 & -\frac{\bar{q}_o}{\bar{v}} \end{bmatrix}, \boldsymbol{B} = \begin{bmatrix} 1 & 1 & -1 & 0 \\ \frac{\bar{\rho}_i - \bar{\rho}}{\bar{v}} & \frac{1-\bar{\rho}}{\bar{v}} & 0 & \frac{\bar{q}_o}{\bar{v}} \end{bmatrix}, \textit{and } \boldsymbol{C} = \begin{bmatrix} 1 & 0 \\ 0 & 1 \end{bmatrix}.$$

3.4. Model Predictive Control

The MPC controller can be described as:

$$\begin{aligned} &\min_{u_{k|k},\ldots,u_{k|k+N_c}} J\left(u, x_{k|k}\right) \\ &\text{s.t.} \\ &x \in \mathcal{X} \triangleq \left\{ x \in \mathbb{R}^{N_x \times N_p} \middle| \, x_l \le x \le x_h \right\} \\ &u \in \mathcal{U} \triangleq \left\{ u \in \mathbb{R}^{N_u \times N_c} \middle| \, u_l \le u \le u_h \right\} \\ &y \in \mathcal{Y} \triangleq \left\{ y \in \mathbb{R}^{N_y \times N_p} \middle| \, y_l \le y \le y_h \right\} \\ &x(k|k) \triangleq \text{Initial state} \\ &\left.\begin{aligned} x_{k+i+1|k} &= f\left(x_{k+i|k}, u_{k+i|k}\right) \\ y_{k+i|k} &= h\left(x_{k+i|k}, u_{k+i|k}\right) \end{aligned}\right\} \forall i = 1, 2, ..., N_c \\ &\left.\begin{aligned} x_{k+i+1|k} &= f\left(x_{k+i|k}, u_{k+N_c|k}\right) \\ y_{k+i|k} &= h\left(x_{k+i|k}, u_{k+N_c|k}\right) \end{aligned}\right\} \forall i = N_c+1, N_c+2, ..., N_p \end{aligned} \quad (14)$$

where N_p is the prediction horizon, N_c is the control horizon. The cost function is defined as:

$$J(\cdot) = \sum_{i=1}^{N_p} \left\| y_{sp} - y_{k+i|k} \right\|_Q^2 + \sum_{i=1}^{N_c} \left\| \Delta u_{k+i|k} \right\|_R^2 \quad (15)$$

where y_{sp} is the controlled variable set-points, and Q and R are the controlled and manipulated variable weighting matrices respectively.

3.5. Linear vs non-linear

Recall that the linear model in (13) was derived on the assumption that higher order, non-linear, terms in (7) can be disregarded since, close to the nominal operating point $\bar{x}$, higher order terms will be approximately zero. Processes, of course, continuously deviate from their nominal operating point, and inaccuracies arising from linear model approximations can not be avoided. These inaccuracies between true system dynamics and those predicted by the model is generally revered to as model mismatch.

Considering that the vast majority of industrial model predictive control solutions rely on linear models to control non-linear processes (Qin and Badgwell, 2003), there seem to exist a general disregard for model mismatch. This can be explained by noting that it is comparatively cheap to develop linear models, typically by assuming that the linear dynamic responses of the system follows first order with time delay (FOPDT) transients, and by fitting FOPDT models to data obtained from step testing. Compared to a first principles approach to obtain a non-linear model a linear model obtained from step tests are markedly less complicated and time consuming. Generally, linear approximations are at least accurate to the direction of relationships between model inputs and outputs. This is considered "good enough" for control since the system can be driven towards a desired operating point. Moreover, the negative effects of some model mismatch is likely never considered when a linear MPC achieves noteworthy improvements compared to the legacy control system.

A linear approximation for this surge tank model would not be sufficient, however, since the observed deviation of input density from the tailings dam would cause inversion of the direction of the relationship between input flow q_i and tank density ρ. Consider that for the linear approximation of the surge tank model, the term in the input matrix $\boldsymbol{B}$ in (13) associated with the input flow q_i will always be positive, since a constant flow of input water q_w is needed to maintain the screen, which would dilute the incoming tailings and guarantee that

$$\frac{\bar{\rho}_i - \bar{\rho}}{\bar{v}} > 0. \tag{16}$$

A linear MPC relying on the model in (13) would therefore always use q_i to increase ρ. However, the re-mining process followed at the tailings dam, described in Section 2, is very unstable and results in an instantaneous input density ρ_i that varies over a large range. This instability often results in a scenario where the direction of the relationship between q_i and ρ would be

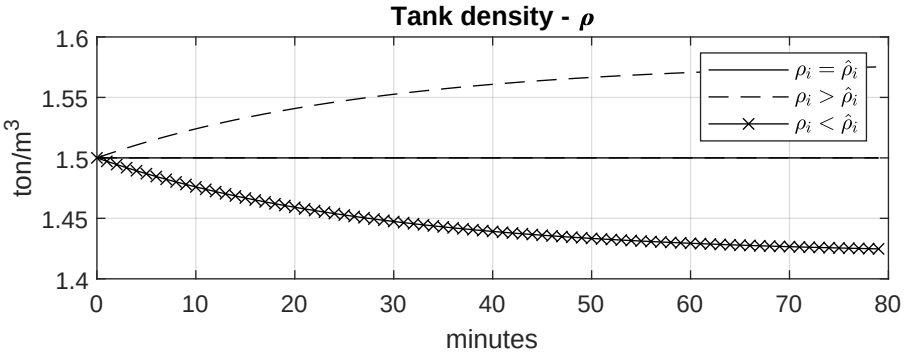

Figure 8: Gain inversion in the relationship between input flow q_i and tank density ρ as a result of significant variance in the instantaneous input density ρ_i.

negative, i.e. an inversely proportional relationship where an increase in q_i would result in a decrease in ρ.

This *gain inversion* is demonstrated in Fig. 8 for a fictitious, although reasonably likely, steady state operating point. Specifically, the steady state operating point is considered for

$$\begin{aligned} &\bar{q}_i = 600,\ \bar{q}_w = 150,\ \bar{q}_o = 750, \\ &\bar{\rho}_i = 1.625,\ \bar{\rho} = 1.5,\ \text{and} \\ &\bar{v} = 350. \end{aligned} \tag{17}$$

Fig. 8, simulates three scenarios using the non-linear model in (5). For all three, the instantaneous input flow q_i remain constant and equal to the steady state input flow $\bar{q}_i$. In the first scenario $(-)$, the instantaneous input density ρ_i remains constant and equal to the steady state input density $\bar{\rho}_i$. In the second scenario $(--)$, $\rho_i = \bar{\rho}_i + 0.1$. In the third scenario $(-\times)$, $\rho_i = \bar{\rho}_i - 0.1$.

Therefore, for a particular control scenario where, where the controller is tasked to maintain the ρ at a target density ρ_{target}, with

$$\begin{aligned} &\rho_i < \bar{\rho}_i \\ &\quad \text{and} \\ &\rho < \rho_{target}, \end{aligned} \tag{18}$$

a linear model based controller would increase q_i, further driving ρ away from ρ_{target}. To avoid this, a non-linear MPC controller was chosen to be implemented.

4. Non-Linear Model Predictive Control

MPC is an advanced control technique which has been put to use extensively in the process control industry (**?**; **?**), and has also received much attention from the academic community (**?**; **?**). The concept of MPC involves the optimisation of a performance function subject to the plant dynamics as well as constraints on the input and output variables over some finite prediction horizon. This process is repeated at each sampling period. This can be expressed in mathematical terms as follows.

$$\min_{\mathbf{u},\delta} \quad V(\mathbf{x}, \mathbf{u}, \boldsymbol{\delta}, \mathbf{y}_{ref}(k))$$

subject to

$$\mathbf{x}(j+k+1|k) = \mathbf{f}(\mathbf{x}(j+k|k), \mathbf{u}(i+k|k))$$
$$\mathbf{y}(j+k|k) = \mathbf{g}(\mathbf{x}(j+k|k), \mathbf{u}(i+k|k))$$
$$\mathbf{x}(k|k) = \mathbf{x}_0$$
$$\mathbf{u}_{min} \leq \mathbf{u}(i+k|k) \leq \mathbf{u}_{max}$$
$$\mathbf{y}_{min} - \boldsymbol{\delta}(k) \leq \mathbf{y}(j+k|k) \leq \mathbf{y}_{max} + \boldsymbol{\delta}(k)$$
$$k = \text{Present sampling instant.}$$
$$j = 0, 1, ..., N_p - 1$$
$$i = 0, 1, ..., N_c - 1$$
$$N_p \geq N_c \times N_b$$
$$\mathbf{x} \in \Re^{N_x \times N_p}$$
$$\mathbf{u} \in \Re^{N_u \times N_c}$$
$$\mathbf{y} \in \Re^{N_y \times N_p}$$
$$\boldsymbol{\delta} \in \Re^{N_y}$$

where N_x is the number or states, N_u is the number of control inputs, N_y is the number of outputs, N_p is the number of predictions in the prediction horizon, N_c is the number of control moves to be calculated in the optimisation

problem, N_b is the number of subsequent samples the control move is kept constant during predictions and $\mathbf{x}_0$ is the value of the state at the present sampling time. The performance index V typically takes on a quadratic form such as:

$$\begin{aligned} &V(\mathbf{u}, \mathbf{x}, \boldsymbol{\delta}, \mathbf{y}_{ref}(k)) = \\ &\sum_{j=1}^{N_p} (\mathbf{y}_{ref}(k) - \hat{\mathbf{y}}(k+j|k))^T \mathbf{Q} (\mathbf{y}_{ref}(k) - \hat{\mathbf{y}}(k+j|k)) \\ &+ \sum_{i=1}^{N_c} \Delta\mathbf{u}(i+k|k)^T \mathbf{R} \Delta\mathbf{u}(i+k|k) + \boldsymbol{\delta}(k)^T \boldsymbol{\Psi} \boldsymbol{\delta}(k) \end{aligned} \tag{19}$$

where matrices $\mathbf{Q}$, $\mathbf{R}$ and $\boldsymbol{\Psi}$ are diagonal matrices used to weight the importance of the different input, output and slack variables which in turn adjusts the behaviour of the controller. $\hat{\mathbf{y}}$ indicates the predicted values of the process output and:

$$\mathbf{y}_{ref} \in \Re^{N_y}$$

$$\mathbf{Q} \in \Re^{N_y \times N_y}$$

$$\mathbf{R} \in \Re^{N_u \times N_u}$$

$$\boldsymbol{\Psi} \in \Re^{N_y \times N_y}$$

$$\Delta\mathbf{u}(i) = \mathbf{u}(i+k|k) - \mathbf{u}(i+k-1|k)$$

At each sampling instant a measurement of the system state $\mathbf{x}_0$ is taken. The measured state is then used as an initial condition for model predictions to be performed as part of the optimisation procedure. The specified number N_c of control vectors as well as the vector of slack variables $\boldsymbol{\delta}$ are the decision variables in the optimisation procedure. The input column vectors of $\mathbf{u}$ are used to simulate the plant model (either nonlinear or linear) with N_b denoting the number of subsequent time steps the input vector is kept constant. The vector of slack variables $\boldsymbol{\delta}$ is used as a decision variable in the optimisation with the purpose of implementing soft constraints on the output variables. This allows the output to violate the constraints at times with the slack variables used to drive them back slowly to within the constraints. Hence the elements in the weighting matrix $\boldsymbol{\Psi}$ are typically large. The solution produces N_c control vectors which can be denoted as $\tilde{\mathbf{u}}$. The first vector in $\tilde{\mathbf{u}}$, that is $\tilde{\mathbf{u}}(0)$ is implemented on the plant at the beginning of the next time

step, when a new measurement of the state is taken and the optimisation process is repeated.

It is often the case that not all the states in $\mathbf{x}$ are measurable, which has given rise to the necessity of state estimation by the use of some form of state observer. In this case it is not necessary as the states in both the linear and nonlinear state-space models in (**??**) and (**??**) are the same as the outputs of the system and are measurable.

The MPC problem formulation described will provide off-set free reference tracking, provided that the model is an ideal representation of the plant (**?**). If there is any plant model mismatch or unmeasured disturbances, steady state off-set will result due to differences in the model predictions and actual plant behaviour. The input density ρ_i is not available to the controllers, and is thus an unmeasured disturbance. In order to correct for this, some type of integral mechanism needs to be included in the controller.

5. Controller Design and Simulation

A Under this scenario, ρ can be maintained closer to ρ_{target}, by decreasing the input allowing the tank level l to

6. Controller Implementation and Evaluation

References

Craig, I.K., 1997. On the role of the general control problem in engineering education, in: 4th symposium on advances in control education, IFAC, London. p. 241–244.

Craig, I.K., Henning, R.D.G., 2000. Evaluation of advanced industrial projects: a framework for determining economic benefit. Control Engineering Practice 8, 769–780.

Dontsov, E.V., Perice, A.P., 2014. A new technique for proppant schedule design. Hydraulic Fracturing Journal 1.

Holland-Batt, A.B., Balderson, G.F., Cross, M.S., 1982. The application and design of wet-gravity circuits in the south african minerals industry. SAIMM .

Ntengwe, F., Witika, L.K., 2011. Optimization of the operating density and particle size distribution of the cyclone overflow to enhance the recovery of flotation of copper sulphide and oxide minerals. SAIMM .

Qin, S.J., Badgwell, T.A., 2003. A survey of industrial model predictive control technology. Control Engineering Practice 11, 733–764.

Seborg, J.E., Edgar, T.F., Mellichamp, D.A., III, F.J.D., 2011. Process dynamics and control. John Wiley and Sons. chapter 3.4. 3 edition. p. 49.

Skogestad, S., Postlethwaite, I., 2005. Muuultivariable feedback control: analysis and design. John Wiley and Sons. 2 edition.